Journal of Applied Fluid Mechanics, Vol. 18, No. 12, pp. 3006-3017, 2025.
Available online at www.jafmonline.net, ISSN 1735-3572, EISSN 1735-3645.
.https://doi.org/10.47176/jafm.18.12.3642

Thermal Performance of Two-phase Loop Thermosiyphon under Different Filling Ratios and Heat Transfer Distances

Y. Yang, Y. Liu, Z. Yan† and Z. Jiang

Shanghai Institute of Technical Physics, Chinese Academy of Sciences, Shanghai 200083, China

†*Corresponding Author Email: yanzhe@mail.sitp.ac.cn*

ABSTRACT

To address the thermal challenges of electronic chips in an energy-efficient manner, this study proposes an optimized two-phase loop thermosiyphon (TPLT) system featuring a mini-channel evaporator, finned condenser, and flexible tubing. This design ensures reliable performance over extended distances while accommodating high heat fluxes and complex cooling scenarios. The effects of filling ratio and heat transfer distance on thermal performance were systematically investigated. Experiments were conducted under controlled ambient conditions of 20°C and 40% relative humidity. To minimize radial heat losses and ensure measurement accuracy, a layered insulation system was implemented, consisting of alternating wraps of thermal insulation wool and plastic packaging. Results demonstrate that the thermosiyphon's performance is highly dependent on the filling ratio, with thermal resistance initially decreasing before rising as the filling ratio increases. Under high heating power conditions, the system achieved a remarkably low thermal resistance of 0.004 K/W. The maximum heat transfer capacity reached 800 W, underscoring the system's robust performance. Notably, when the heat transfer distance was extended from 3.7 m to 5.7 m, thermal resistance increased only marginally, while the heat transfer limit decreased by a mere 50 W, confirming the system's exceptional suitability for long-distance heat dissipation. These findings offer significant insights for thermal management in advanced electronic devices, demonstrating the potential of the proposed TPLT design as an efficient and scalable cooling solutions for high-power applications.

Article History

Received April 30, 2025
Revised July 18, 2025
Accepted July 27, 2025
Available online October 6, 2025

Keywords:

Thermosiyphon
Mini-channel evaporator
High-power
Long distance
Thermal resistance

1. INTRODUCTION

With the rapid development of electronic technology, the integration density of electronic components continues to increase, leading to a corresponding rise in heat flux density (Hu et al., 2023). Effective thermal management is critical for ensuring the performance and lifespan of electronic components (Naik et al., 2013; Sakthivel et al., 2018), while energy-efficient cooling solutions remain a key priority. The common types of heat pipes include grooved heat pipes (Jiao et al., 2007), loop heat pipes (Liu et al., 2023), pulsating heat pipes (Cheng & Wong, 2024), and thermosiyphons (Srivastava et al., 2024). Among these, grooved heat pipes rely on capillary structures to drive working fluid reflux, featuring simple construction and high reliability. Loop heat pipes (LHPs) utilize capillary pressure generated by the evaporator wick to circulate the working fluid, exhibiting superior long-distance heat transfer capability and excellent anti-gravity performance. Pulsating heat pipes (PHPs) operate without capillary structures, demonstrating simple configuration and high heat flux capacity. Unlike pump-driven systems, two-phase loop heat pipes employ passive heat transfer mechanisms, combining structural simplicity, high efficiency, and energy-saving advantages, making them a focus of recent research.

Most existing studies on two-phase loop heat pipes focus on capillary wick-based designs, with several efforts to optimize heat transfer distance. Bai et al. developed a dual-compensation chamber LHP with a 2.2 m heat transfer distance, finding that evaporator liquid/vapor composition and heat leakage significantly impacted startup performance (Bai et al., 2009). Adoni et al. (2010) designed an ammonia stainless steel disc-shaped LHP with a nickel wick and 1760 mm transfer distance, achieving a 300 W maximum heat load and observing a distinctive "√"-shaped temperature trend. Maydanik & Vershinin (2009) reported cylindrical LHPs using

ammonia, attaining a 110 W maximum heat load and 0.53 K/W minimum thermal resistance under air cooling. Xu et al. 2020) nintroduced a double-layer composite copper wick to minimize heat leakage at high loads, enabling rapid startup and a 140 W maximum capacity. Nakamura et al. (2022) employed a sub-nanometre porous glass wick (0.1 μm class) to achieve 2 m anti-gravity operation with an 85 W heat load across a 6.5 m vapor line. Cao et al. (2022) fabricated a Ti_3 (Al, Si) C_2 wick with double pore size, demonstrating successful 30 W startup and 0.391 K/W thermal resistance at 140 W.

However, the above-mentioned capillary core loop heat pipes usually have limited heat transfer distance and low heating power, making them unsuitable for the high heating power cooling needs of microelectronic devices/data centers. The two-phase loop thermosiyphon, also known as separated gravity heat pipe, is a passive heat transfer device with high heat transfer (Vasiliev et al., 2022; Venkataramana et al., 2022). Leveraging gravity-driven operation, they are promising for high-power, long-distance applications.

Sarno et al. (2013) evaluated the maximum heating power of an R141b-charged loop Thermosiyphon at a 20° tilt angle, achieving 100 W a significant improvement over conventional aircraft cooling systems. Samba et al. (2013) demonstrated the superior performance of a Thermosiyphon-based cooling system for France Telecom cabinets, meeting ETSI specifications. While traditional systems were limited to around 250 W, the Thermosiyphon system handled up to 600 W. Jengsooksawat et al. (2014) investigated heating power limits in a steam-chamber loop Thermosiyphon across different working fluids at optimal filling ratios: 600 W (water), 900 W (ethanol), and 1200 W (R-11). Agostini et al. (2014) introduced a two-phase Thermosiyphon cooler for power electronic devices, which achieved a total thermal resistance of 40~50 K/kW within a power loss range of 500~1500 W. Matsubara et al. (2014) tested a Thermosiyphon circuit using water as the working fluid, installed four types of core blocks in the evaporator, and found that the maximum heating power was 400 W. Zimmermann & Melo (2014) studied CO_2 Thermosiyphons by varying heat source-radiator temperatures, refrigerant charge, and evaporator airflow rate, achieving a 514 W heating limit. Chen & Yang (2016) designed an annular Thermosiyphon heat sink for HCPV cooling, identifying acetone as the optimal working fluid (199.5 W max power) through fin-structure optimization. Zhang et al., (2017) proposed the "ideal cycle" and developed a visualization experimental platform to evaluate the performance of two-phase Thermosiyphons. Under the ideal cycle, the performance reaches its optimum when the filling ratio is 100% and the heat transfer height difference is 1.2 m. Zhang et al. (2020) conducted experimental research on the dual evaporator circuit Thermosiyphon and analyzed the influence of heating power distribution on start-up time and overshoot. The maximum heating power obtained was 60 W. Kloczko & Faghri (2020) proposed a coreless non phase change heat pipe (NPCHP) with thermal resistance of 0.0165~0.0256 K/W (90% filling ratio, 200 W max) and optimal 350 W output at 75~80% filling. Armas et al. (2021) designed a passive loop Thermosiyphon cooling system using R1234ze(E) working fluid, with a maximum heating power of 500W and a thermal resistance of 0.081 K/W. The system was validated using an internal simulator with an error rate of only 2.1%. Cataldo & Crea (2021) proposed a model of a Thermosiyphon using machine learning methods. Using R1234ze(E) working fluid, the maximum heating power of a single fan condenser is 330 W, and the maximum heating power of a dual fan condenser is 570 W. He et al. (2022) conducted visible experimental studies on small-diameter annular Thermosiyphons with a wide filling ratio range (44~97%). The maximum heat transfer capacity was found to increase first and then decrease with the increase of filling ratio. At high filling ratios (73% and 82%), vapor-liquid flow transitions to slug flow, intermittent spring boiling, and bubble flow. The diameter of the bubbles gradually decreases with increasing heat load, and the maximum heat transfer can reach 280 W. Hua et al. (2024) conducted experimental research on the start-up and heat transfer characteristics of a reservoir auxiliary loop Thermosiyphon (MGTPLT) with a microgroove evaporator, and compared it with a loop Thermosiyphon (STPLT) with a smooth tube evaporator. It was found that MGTPLT has a shorter start-up time and exhibits better temperature uniformity, achieving 250 W heat transfer at moderate filling ratios. Zamanifard & Melo (2024) proposed a novel remote loop Thermosiyphon (RLTS) for high heat flux applications and cooling 2U servers, and evaluated key factors such as fill ratio, air flow rate, and heat load. It was found that the Thermosiyphon can effectively manage a heating power of 640 W at an intake temperature of 28°C and an airflow velocity of 170 cubic feet.

In summary, existing studies on loop Thermosiyphon have primarily focused on systems with heat transfer distances below 3 m and heating powers under 500 W. In addition, the simple tubular evaporator structure constrains the coupling effect with planar heat source. In view of this, this study designed and prepared a long-distance two-phase loop Thermosiyphon with mini-channel evaporator, and explored the effects of filling ratio and heat transfer distance on the thermal performance of the two-phase loop Thermosiyphon. This design effectively solves the needs of high heating power and high heat flux heat dissipation, providing important reference for the efficient and energy-saving cooling field of microelectronic devices.

2. Design and Experimental System of Two-phase Loop Thermosiyphon with Mini-channel Evaporator

2.1 Design of Two-phase Loop Thermosiyphon with Mini-Channel Evaporator

To meet the requirements of high heating power and long-distance heat transfer, we designed a two-phase loop Thermosiyphon system.

The mini-channel evaporator is the core component of a two-phase loop Thermosiyphon, consisting of upper and lower manifolds and mini-channels. The evaporator shell material is aluminum, the inner diameter of the tube

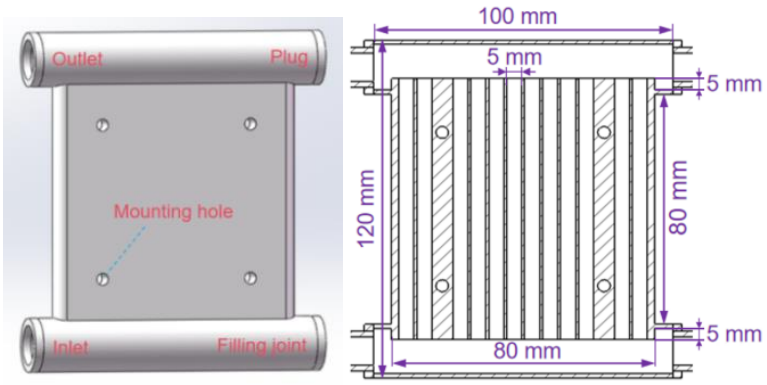

Fig. 1 Mini-channel evaporator (a) model (b) dimensions

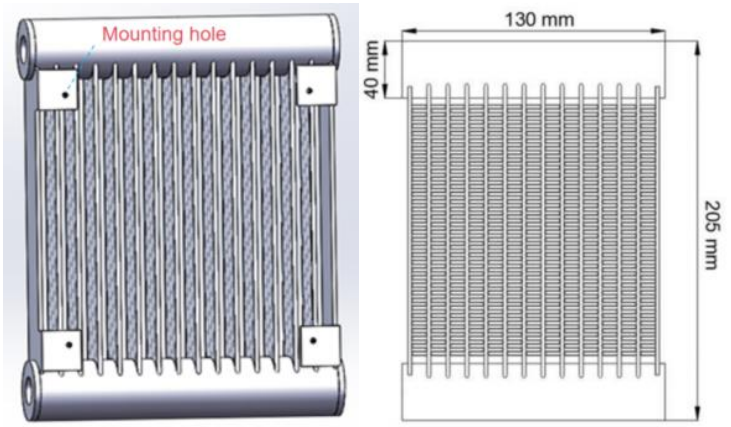

Fig. 2 Fin tube condenser (a) model (b) dimensions

is 5 mm, the number of mini-channels is 12, and the depth of the mini-channels inserted into the upper and lower headers is 5 mm. The model and dimensions are shown in Fig. 1. This heat pipe is connected with multiple clamps. For operational safety, we established 1.4 MPa as the maximum internal pressure limit. When this pressure threshold is reached, the system is considered to have attained its maximum heat transfer capacity, and no further heating power increase is permitted.

This work employs a typical finned tube condenser, with its model and dimensions illustrated in Fig. 2. The condenser incorporates a square DC fan, secured by four mounting holes. Its width and height measure 130 mm and 205 mm, respectively, and it contains 14 flat tubes, each featuring 15 mini-channels.

The two-phase loop Thermosiyphon tube designed in this work is composed of stainless steel bellows and aluminum tube, as shown in Fig. 3. The flexibility of the stainless steel bellows enables the system to accommodate long-distance heat transfer and adapt to complex thermal environments. To meet the technical requirement of a heat transfer distance of no less than 5 m, a tube with an inner diameter of 10 mm was selected. The height difference within the system serves as the primary driving force for the Thermosiyphon operation.

2.2 Filling of Working Fluid

The filling ratio of the working fluid is defined as the ratio of the volume of liquid filled to the total volume

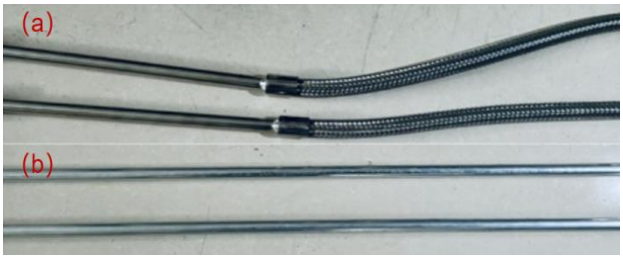

Fig. 3 Diagram of connection pipe: (a) Stainless steel bellows; (b) Aluminum tube

inside the two-phase loop Thermosiyphon, expressed as follows:

$$\alpha = \frac{V_l}{V} \times 100\% \tag{1}$$

In the formula, α represents the filling ratio, V_l represents the volume of liquid filled, V represents the total volume inside the Thermosiyphon.

However, in practical operation, the filling ratio is usually calculated by calculating the actual filling mass, and the calculation formula is as follows:

$$m = m_{\mathrm{l}} + m_{\mathrm{v}} = \alpha\rho_{\mathrm{l}}V + (1-\alpha)\rho_{\mathrm{v}}V \tag{2}$$

In the formula, m represents the filling mass, and subscripts l and v represent liquid and vapor, respectively.

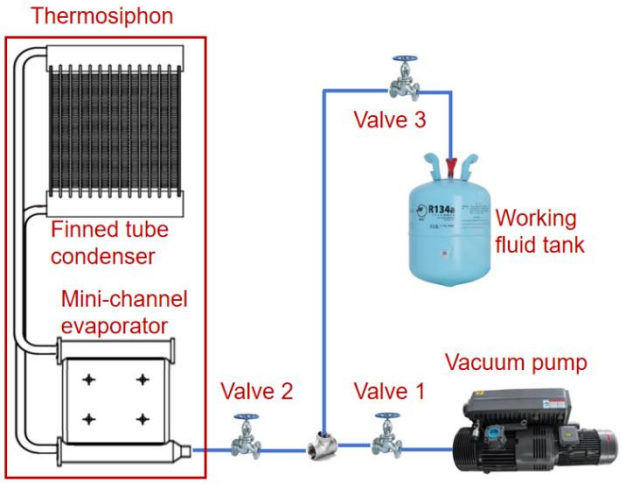

Fig. 4 Schematic diagram of filling system

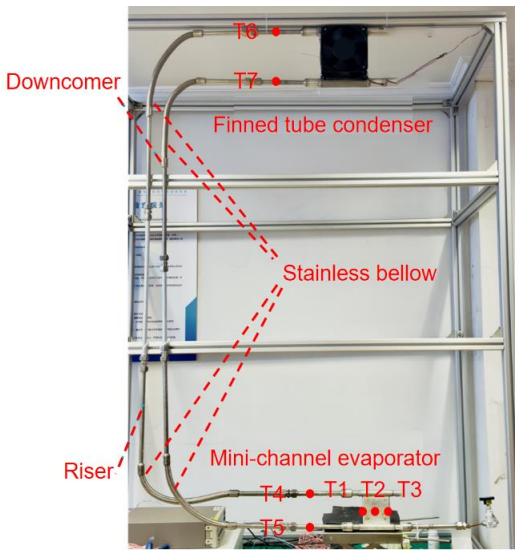

Fig. 5 Layout of long-distance two-phase loop Thermosiyphon and temperature measurement points

In practical calculations, the last term is usually ignored because the vapor density is much lower than the liquid density at the same pressure.

Confirm the filling amount and use the filling system shown in Fig. 4 to fill the Thermosiyphon. Prior to working fluid charging, thermosiyphons require a baking degassing process to thoroughly remove contaminant gases from the internal components. The filling system mainly consists of a vacuum unit, valves, pipelines, Thermosiyphon, and working fluid tanks. The working fluid filling system designed in this article utilizes pressure and gravity differences to inject the working fluid into the Thermosiyphon. The actual filling mass is the total mass after the completion of the Thermosiyphon filling minus the mass before the Thermosiyphon filling.

R134a is selected as the working fluid for the heat pipe due to its favorable thermophysical properties and practical advantages. Specifically, R134a exhibits a relatively high latent heat of vaporization, which significantly enhances the heat transfer efficiency of the heat pipe. Additionally, its low viscosity and high thermal conductivity facilitate fluid flow and phase-change heat transfer. Furthermore, R134a is environmentally friendly and cost-effective, making it a practical choice for widespread applications.

2.3 Experimental System

The prototype of a long-distance flexible two-phase loop Thermosiyphon is shown in Fig. 5, which includes a mini-channel evaporator, finned tube condenser, riser, downcomer, and metal bellows. The Thermosiyphon circuit is suspended using an aluminum alloy bracket structure and wrapped with insulation material to reduce environmental heat leakage and improve the accuracy of experimental results (to enhance the display effect, the schematic diagram does not include multiple insulation layers wrapped around it). A platinum-resistance temperature sensors (PT1000, Model WZP) was employed for temperature sensing. There are 3 PT1000 temperature sensors attached to the evaporator, and temperature sensors are also attached at the inlet and outlet of the evaporator and condenser, totaling 7 sensors.

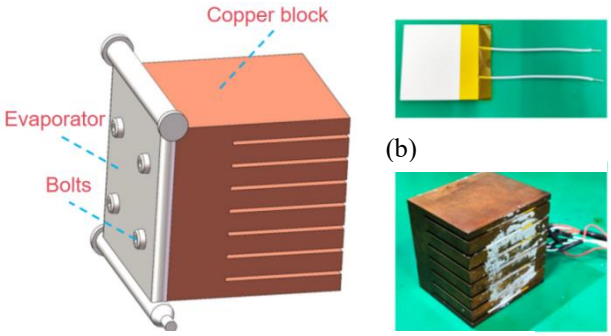

Fig. 6 Heating configuration in the experiment using the ceramic heating element strategy: (a) the diagrammatic sketch for the combination of the evaporator and copper block, (b) the single ceramic heating element, and (c) the copper block

Figure 6 presents the heating configuration in the experiment using the ceramic heating element strategy. To achieve the high-power heating, the copper block is designed. Seven ceramic heating elements are contained in the copper block,and the maximum power for each ceramic heating element is about100W. I addition, owing to the high thermal conductivity of copper material (397 W/m·K), a uniform heat flux could be achieved. The tight combination of the evaporator and copper block is achieved by means of bolts. It should be also noted that to lower the thermal resistance in the heating module, the gaps between the copper block and ceramic heating element, as well as the evaporator, are configured with thermal grease.

In the thermal performance testing of Thermosiyphon, a multilayer composite insulation structure is employed to minimize heat exchange between the system and the environment. Initially, a high-thermal-resistance insulation wool is wrapped around the Thermosiyphon as the primary thermal barrier, followed by an airtight plastic

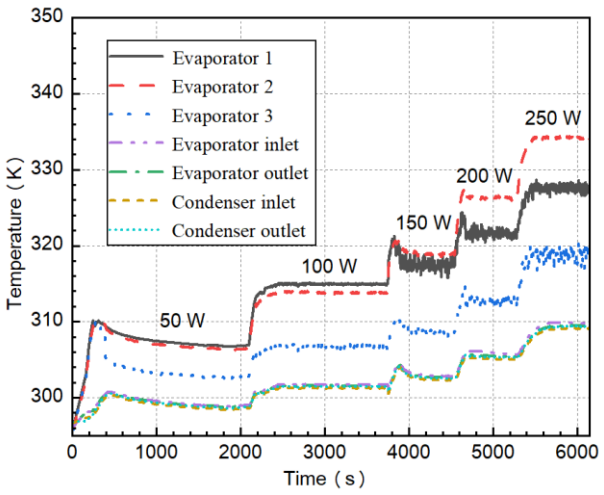

Fig. 7 Variation of temperature of thermosiyphon with heating power at 50% filling ratio

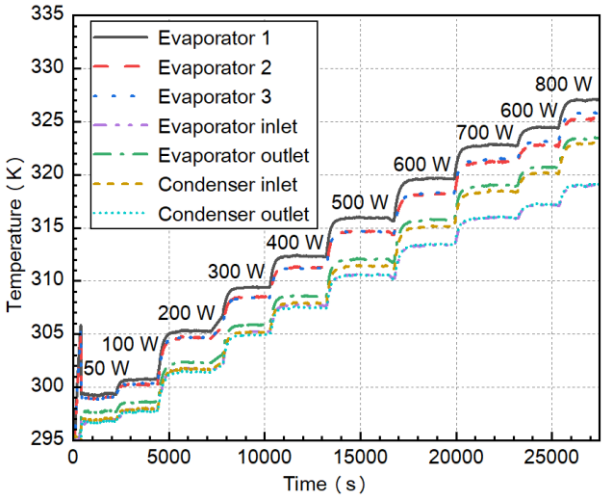

Fig. 8 Variation of temperature of thermosiyphon with heating power at 70% filling ratio

film to suppress convective heat transfer. Subsequently, a second layer of insulation wool and plastic film is applied in an alternating arrangement. This layered insulation approach effectively reduces radial heat loss from the test system, thereby ensuring the accuracy of experimental data.

3. Results and Discussions

To provide a detailed explanation of the effects of filling ratio and heat transfer distance on thermal performance, corresponding experimental studies were conducted.

3.1 The Influence of Filling Ratio on Thermal Performance

The heat transfer distance of the two-phase loop Thermosiyphon is 1.6 m, and three representative filling ratios of medium (50%), high (70%), and extremely-high (95%) are selected for research. The cooling power is fixed at 5 W.

3.1.1 Thermal Performance at Medium Filling Ratio of Medium (50%)

Figure 7 shows the temperature variation characteristics of a two-phase loop Thermosiyphon under the condition of 50% filling ratio as the heating power gradually increases.

As the heating power gradually increases from 50 W to 250 W, the temperature at each measuring point shows an overall upward trend, but the heating process and steady-state characteristics exhibit obvious step like changes. At an initial 50 W power input, the evaporator temperature rapidly rises to around 310 K before experiencing a slight decrease and subsequent stabilization. At this point, the system is in a dominant state of vapor-phase latent heat transfer, and the bubbles generated by the evaporator liquefy after reaching the condenser through the riser, completing the heat transfer cycle. Notably, except for the evaporator, the temperatures at other measuring points are relatively close, indicating that the working fluid is basically in a saturated state after flowing out of the evaporator, and the saturation pressure change inside the condenser is relatively small.

When the heating power is increased to 100 W and 150 W, the system exhibits significant transition characteristics. Notably at 150 W, evaporator measurement point 1 began to show significant fluctuations with an amplitude of about 3 K. When power reaches 200 W, the oscillation amplitude diminishes to 2 K. At the maximum tested power of 250 W, the evaporator temperature approaches the upper limit of the working temperature range of the working fluid (about 335 K), and the temperature fluctuation amplitude decreases to 1 K. At low power (50 W and 100 W), the liquid evaporation at the hot end is smooth and the steam flow is stable. At power (150 W, 200 W, 250 W), the increase in heat flux density may lead to a transition from nucleate boiling to film boiling, with local drying and rewetting alternating, causing temperature oscillations. Furthermore, similar phenomena have been observed in heat pipe studies by Holman et al. (2020), Guo et al. (2020), and Rukruang et al. (2024), where increased heat flux under high thermal loads was found to induce flow instabilities and trigger thin-film boiling, ultimately leading to localized dryout phenomena (Holman et al., 2020; Guo et al., 2020; Rukruang et al., 2024). At the same time, the temperature distribution on the evaporator wall is uneven, resulting in significant oscillations at measuring points 1 and 3 of the evaporator, while measuring point 2 of the evaporator is relatively stable.

The experimental results indicate that the two-phase loop Thermosiyphon with a medium filling ratio of 50% is not suitable for high heating power heat transfer scenarios.

3.1.2 Thermal Performance At High Filling Ratio of High (70%)

Figure 8 presents the temperature evolution of a two-phase loop Thermosiyphon with a 70% filling ratio under progressively increasing heating power (50 W to 800 W) over a 25000-second experimental duration.

It is worth noting that there is a significant temperature stratification phenomenon between different measuring points. The measuring point of evaporator 1 always maintains the highest temperature, gradually increasing from about 299 K at 50 W to about 327 K at 800 W. The temperature at the outlet measuring point of the condenser is the lowest, rising from an initial temperature of about 297 K to about 319 K. This temperature difference is mainly due to the thermal resistance and flow characteristics of the working fluid during the heat transfer process. The evaporator area serves as the heat input end and directly receives the heat load, resulting in the highest temperature. As the working fluid flows through various components of the system, it gradually releases heat, causing the temperature of the measuring points to decrease sequentially.

The temperature gradient between measurement points exhibits a positive correlation with heating power, increasing from 3.27 K at 50 W to approximately 6.34 K at 800 W. This thermal response becomes particularly pronounced in the high-power regime (600~800 W), which is mainly attributed to the high liquid filling ratio (70%) conditions where there is more liquid in the condenser, limiting the effective heat transfer area between the vapor phase and the tube wall. At the same time, under high heating power driving, the circulation speed of the working fluid is accelerated, which reduces the residence time of the working fluid in the condenser, resulting in a decrease in condensation efficiency and a continuous increase in the outlet temperature of the condenser.

The temperature transient characteristics at different power levels reveal several important phenomena (Fig. 8). During initial low-power operation (50 W), the system temperature exhibits a brief overshoot phenomenon, while during the subsequent heating power increase process, the temperature changes tend to stabilize. As the heating power increases, the time required for the system to reach thermal equilibrium is shortened, indicating that the thermal response speed of the system is faster under high heating power conditions, thanks to the enhanced driving force of vapor-liquid two-phase flow, which improves the heat transfer efficiency.

The experimental results indicate that the two-phase loop Thermosiyphon with a high filling ratio of 70% is suitable for high heating power heat transfer scenarios.

3.1.3 Thermal Performance at Extremely-High Filling Ratio of Extremely-High (95%)

Figure 9 shows the temperature variation characteristics of a two-phase loop Thermosiyphon under 95% filling ratio conditions as the heating power gradually increases.

At a 95% filling ratio, the evaporator temperature (evaporators 1, 2, 3) gradually increased from an initial value of about 296 K to about 332 K at a heating power of 500 W, demonstrating good temperature response characteristics. It is worth noting that there are significant temperature differences between different measuring points in the Thermosiyphon system. The temperature at the evaporator measuring point is always higher than other

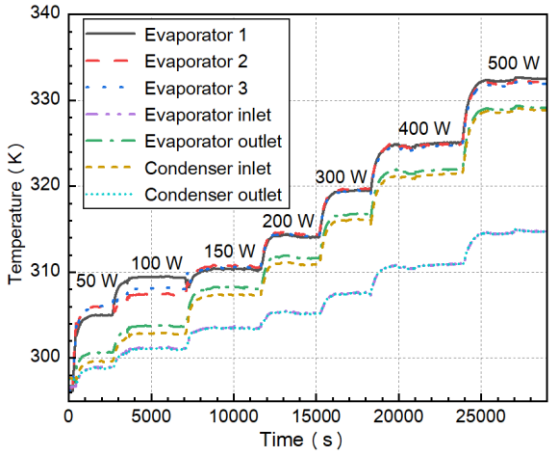

Fig. 9 Variation of temperature of thermosiyphon with heating power at 95% filling ratio

parts of the system, while the outlet temperature of the condenser is maintained at the lowest level. This temperature gradient clearly reflects the heat transfer path in the system.

The temperature difference between the inlet and outlet of the evaporator and condenser progressively widens with increasing heating power, particularly above 150 W. The formation of this phenomenon is mainly attributed to the limited vapor-phase space inside the Thermosiyphon under high liquid filling ratio, which leads to the gradual transition of the system from two-phase flow boiling heat transfer to single-phase natural convection heat transfer. The temperature difference between the inlet and outlet of the evaporator increased from about 6.60 K at 50 W to about 17.21 K at 500 W, while the condenser exhibits a comparable trend. The expansion of this temperature difference reflects the characteristics of a decrease in the flow rate of the working fluid inside the Thermosiyphon and a decrease in heat transfer efficiency.

Notably, the temperature distribution across the three evaporator measurement points reveals initial disparities at low heating powers (50 W and 100 W), where the temperature of Evaporator 1 deviates from those of Evaporators 2 and 3, with a maximum observed difference of 2.01 K. This unevenness is mainly due to the differences in the degree of phase transition in each channel of the evaporator under high filling ratio conditions, as well as the resulting fluctuations in local heat transfer efficiency. As the heating power increases, the temperatures at the three points become similar, indicating a uniform distribution of heat load. At 500 W, the system attains a peak temperature of approximately 332 K. Given that liquid expansion at this stage risks generating excessive internal pressure inside the tube, the Thermosiyphon approaches its operational limit for the current filling ratio.

3.1.4 The Influence of Filling Ratio on Thermal Resistance Characteristics

System thermal resistance is an important indicator for measuring the thermal performance of a two-phase

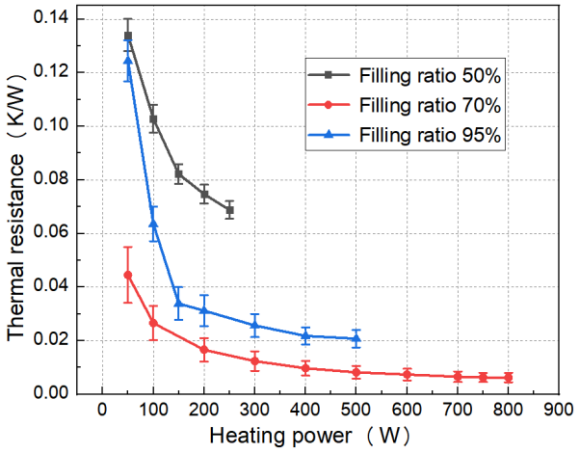

Fig. 10 Variation of thermal resistance at 1.6 m heat transfer distance

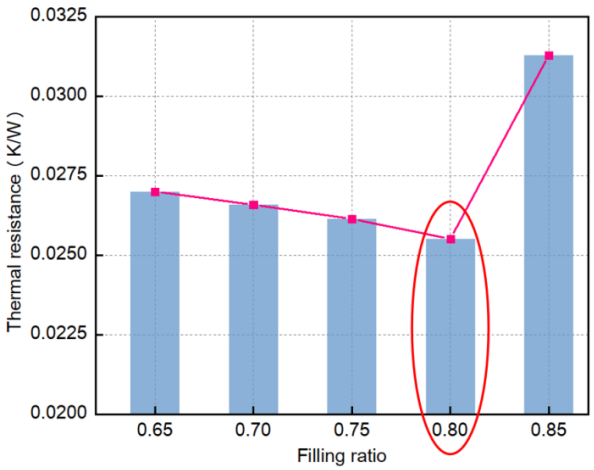

Fig. 11 Thermal resistance at different filling ratio

loop Thermosiyphon. The system thermal resistance is defined as:

$$R = \frac{\overline{T_{\text{eva}}} - T_{\text{amb}}}{Q_{\text{h}}} \tag{3}$$

In the formula: $\overline{T_{\text{eva}}}$ represents the average temperature of the evaporator; T_{amb} represents the ambient temperature.

Figure 10 illustrates the variation in thermal resistance of the Thermosiyphon system as a function of heating power for different filling ratios.

The experimental results demonstrate that under identical heating power conditions, the system exhibits the highest thermal resistance at a 50% filling ratio, followed by 95%, while the 70% filling ratio yields the lowest values. With the increase of heating power, the thermal resistance under the three filling ratio conditions shows a decreasing trend, and the rate of decrease is relatively fast in the initial stage, and then tends to flatten out. Specifically, the range of thermal resistance variation of the system is 0.069~0.134 K/W at a 50% filling ratio, 0.006~0.045 K/W at a 70% filling ratio, and 0.021~0.128 K/W at a 95% filling ratio.

At the initial heating power of 50 W, the system exhibits comparable thermal resistance values for both 50% and 95% filling ratios. However, with increasing heating power, the thermal resistance reduction becomes markedly more pronounced at 95% filling ratio (83.73%) compared to 50% filling ratio (48.68%). This is mainly because at a 50% filling ratio, the two-phase loop Thermosiyphon mainly relies on latent heat of phase change for heat dissipation, and effective circulation cannot be formed inside the tube, resulting in a lower overall flow rate. In contrast, the 95% filling ratio enables complete internal circulation, where the accelerated condensate return flow promotes efficient heat removal from the evaporator. This enhanced thermal transport mechanism maintains lower evaporator temperatures and drives the more substantial thermal resistance reduction observed at higher filling ratios.

The condition of 70% filling ratio exhibits the optimal thermal performance, with the minimum thermal resistance reaching 0.0063 K/W at a heating power of 800 W, and the thermal resistance decreasing by as much as 85.83%. Compared with a 95% filling ratio, a 70% filling ratio provides a larger vapor phase space, increases the volume of steam generated per unit time, enhances the bubble pump effect, forms a faster circulation velocity in the tube, and ultimately achieves lower system thermal resistance. It is worth noting that when the heating power exceeds 400 W, the change in thermal resistance of the system under the condition of 70% filling ratio is relatively small, indicating that the system is approaching a stable state. This characteristic indicates that the two-phase loop Thermosiyphon is suitable for high heating power heat transfer applications, because at high heating power, the evaporator can quickly generate continuous bubbles, form a stable circulation, and achieve efficient heat transfer.

In summary, the two-phase loop Thermosiyphon demonstrates optimal thermal performance at a 70% filling ratio, exhibiting both the lowest system thermal resistance and superior operational characteristics, particularly in high-power regimes above above 400 W. These findings provide valuable guidance for the design of Thermosiyphons intended for high-heat-flux applications.

In order to determine the optimal filling ratio at a heat transfer distance of 1.6 m, the filling ratio of 65%, 70%, 75%, 80%, and 85% were studied. The experimental results reveal a gradual decrease in thermal resistance as the filling ratio increases from 65% to 80%, followed by a sharp increase when the ratio further rises to 85%. Among them, the thermal resistance is the smallest at 80% filling ratio, only 0.023 K/W.

3.2 The Influence of Heat Transfer Distance on Thermal Performance

At an 80% filling ratio, the thermal performance of the two-phase loop Thermosiyphon was studied by changing the heat transfer distance of the tube at 3.7 m and 5.7 m.

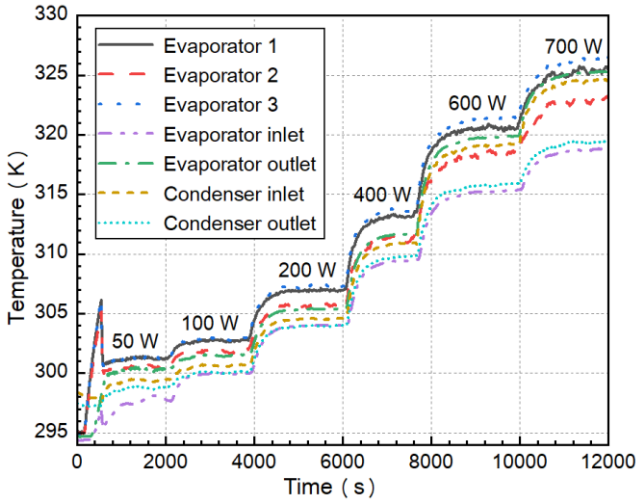

Fig. 12 Temperature variation at 3.7 m heat transfer distance

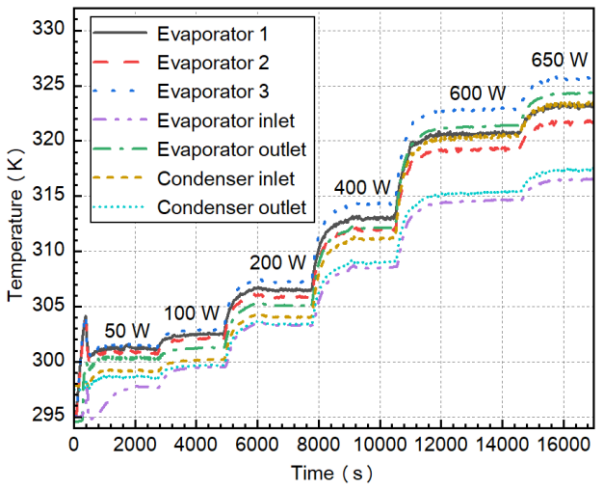

Fig. 13 Temperature variation at 5.7 m heat transfer distance

3.2.1 Heat Transfer Distance of 3.7 m

Figure 12 presents the temperature variation characteristics of a two-phase loop Thermosiyphon under different heating powers at a heat transfer distance of 3.7 m.

The experimental results demonstrate that this configuration reaches its heat transfer limit at 700 W. The temperature profiles reveal a pronounced increasing trend at all measurement points with rising heating power. During system initiation at 50 W, the surface temperature of the evaporator exhibits rapid thermal response characteristics, with the temperature rapidly increasing from an initial 295.08 K to a peak of 306.18 K, and the entire process takes about 390 seconds. This temperature overshoot phenomenon is mainly caused by the transient heat transfer characteristics during the start-up process. It is worth noting that the temperature overshoot value at a heat transfer distance of 3.7 m is 5.43 K, which is less than 6.45 K under the same heating power conditions at a heat transfer distance of 1.6 m. This is mainly attributed to the increase in gravity pressure difference caused by the increase in heat transfer distance, which allows the condensate to flow back to the evaporator in a more timely manner to complete the replenishment process.

With increasing heating power, the temperature difference between the evaporator and condenser gradually widens. Furthermore, the temperature variation among different measurement points (Evaporator 1, 2, 3) becomes more pronounced, particularly under high thermal loads. This is mainly due to the increasing heating power causing the surface temperature distribution of the evaporator to gradually become uneven, and some areas may experience local drying up. At this time, the outlet temperature of the evaporator is basically consistent with the average temperature of the evaporator. This temperature distribution characteristic is due to the increased driving force of the Thermosiyphon under high heating power, which accelerates the reflux speed of the condensate. The bubbles in the mini-channels inside the evaporator can quickly detach from the wall under the shear action of the reflux liquid, preventing heat accumulation inside the evaporator.

3.2.2 Heat Transfer Distance of 5.7 m

Figure 13 presents the temperature variation characteristics of a two-phase loop Thermosiyphon under different heating powers at a heat transfer distance of 5.7 m.

Experimental results reveal that the system achieves a heat transfer limit of 650 W, merely 50 W lower than the 700 W limit observed at 3.7 m. This result fully proves that the system is suitable for high heating power, long-distance heat transfer scenarios. At a heat transfer distance of 5.7 m, when the Thermosiyphon is started at a heating power of 50 W, the evaporator temperature first rapidly rises to a peak of 304.09 K, then suddenly drops due to the reflux of condensate, and finally slowly rises to steady state. It is worth noting that the inlet temperature of the evaporator decreases by 3.33 K, which is the maximum value under the three heat transfer distance conditions. This is mainly attributed to the increased heat transfer distance, which leads to an increase in the height difference between the downcomer and the evaporator, thereby improving the circulation driving force and the flow velocity inside the tube. At the same time, the extension of the downcomer keeps the liquid at the outlet of the condenser in a supercooled state, ultimately resulting in a significant decrease in the inlet temperature of the evaporator.

At heating powers of 200 W, 400 W, 600 W, and 650 W, the maximum temperature difference on the evaporator surface is 0.61 K, 2.12 K, 5.00 K, and 5.96 K, respectively. Under various heating conditions, the temperature at the middle position of the evaporator (evaporator 2) is the lowest, while the temperature at the position far from the inlet (evaporator 3) is the highest, and the difference gradually widens with increasing heating power. This phenomenon indicates uneven flow distribution inside the evaporator, especially in the mini-channel at position 3 where the reflux liquid is not replenished in time and the flow is insufficient, resulting

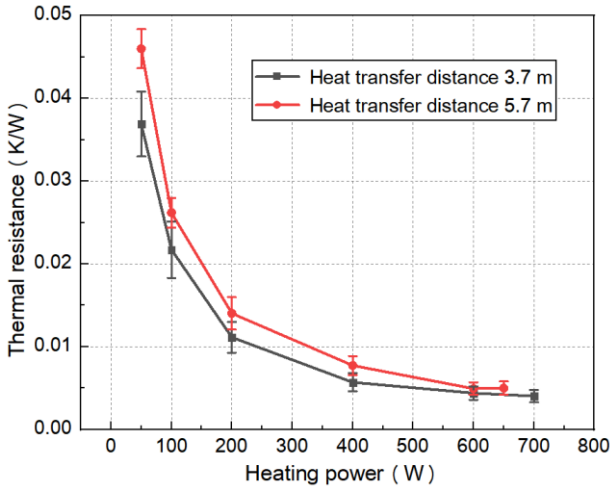

Fig. 14 Variation of thermal resistance at different heat transfer distance

in local drying and causing the wall temperature to rise to the highest level. When the heating power reaches 650 W, the Thermosiyphon reaches the heat transfer limit at that transmission distance. The maximum temperature is close to the upper limit of the system's operating temperature range, so the heating power has not been further increased. This heat transfer limit is only reduced by 7.1% compared to the 3.7 m heat transfer distance, fully verifying the efficient performance of the Thermosiyphon system in long-distance heat transfer.

In summary, compared with a heat transfer distance of 3.7 m, although the total heat transfer capacity is slightly reduced, the system still maintains a high heat transfer efficiency, indicating that the two-phase loop Thermosiyphon has significant advantages in long-distance heat transfer applications.

3.2.3 Comparison of Thermal Resistance Characteristics at Different Heat Transfer Distances

Figure 14 presents the characteristics of the thermal resistance of the two-phase loop thermosiyphon system varying with heating power at different heat transfer distances.

The data shows that under the condition of 3.7 m heat transfer distance, the range of thermal resistance variation of the system is 0.004~0.038 K/W. Under the condition of a heat transfer distance of 5.7 m, the range of thermal resistance variation of the system is 0.005~0.047 K/W. With increasing heating power, the thermal resistance of the system at both distances exhibits a significant decreasing trend. aNotably, the reduction rate is more pronounced in the lower heating power range (50~200 W) than in the higher range (400~700 W), where it gradually stabilizes. This phenomenon is mainly due to the increase in heating power, the evaporation rate of the working fluid increases, the bubble pump effect is enhanced, and the internal fluid circulation of the system is promoted, thereby improving the heat transfer efficiency.

Under low heating power conditions (50 W), the thermal resistance at a heat transfer distance of 5.7 m is 0.008 K/W higher than that at a heat transfer distance of 3.7 m. As the heating power increases to 200 W, this gap narrows to 0.003 K/W. When the heating power reaches 400 W, the difference in thermal resistance between the two further decreases to 0.002 K/W. Under the high heating power condition of 600 W, the thermal resistance values of the two heat transfer distances are almost the same. The phenomenon of decreasing thermal resistance gap with increasing heating power indicates that under high heating power conditions, the impact of longer heat transfer distance on system performance gradually weakens. It is worth noting that although a 5.7 m heat transfer distance theoretically increases fluid resistance, experimental data shows that there is not much difference in thermal resistance in most heating power ranges. This is mainly attributed to the larger gravity potential difference caused by longer heat transfer distances, which enhances the natural circulation driving force of the system, thereby offsetting the adverse effects of increased resistance.

Similar findings regarding thermal resistance have been reported in the field of heat pipes. Srivastava et al. investigated the thermal resistance characteristics of thermosiyphons with horizontal evaporators under low heat flux conditions. Their comparative study of working fluids, including R134a and methanol, revealed that R134a exhibited the lowest thermal resistance during startup, measuring 0.11 K/W (Srivastava, Appl. Therm. Eng., 257 (2024) 124249). Li et al. examined the heat transfer performance of a loop thermosiyphon using n-pentane as the working fluid under high centrifugal forces. They found that the minimum thermal resistance was 0.57 K/W at a filling ratio of 60% and validated its application effectiveness in electric spindle cooling. Compared with the heat pipes reported in the literature, the present system exhibits lower thermal resistance, which is primarily attributed to the enhanced boiling heat transfer facilitated by the mini-channel evaporator (Li et al., 2017). This discovery confirms the superior performance of two-phase loop Thermosiyphons in long-distance, high heating power heat transfer applications, providing important references for the design of thermal management systems.

4. Conclusion and Outlook

In order to meet the growing heat dissipation needs of electronic devices, a flexible two-phase loop Thermosiyphon has been developed and manufactured, which consists of a mini-channel evaporator, a finned condenser, and a flexible pipeline. This study systematically examines the influence of liquid filling ratio and heat transfer distance on thermal characteristics. The principal findings are summarized below:

(1) At a heat transfer distance of 1.6 m, the effects of liquid filling ratios of medium (50%), high (70%), and extremely high (95%) on thermal performance were studied, and it was found that the two-phase loop Thermosiyphon operated better at higher liquid filling ratios. In order to determine the optimal filling ratio at a heat transfer distance of 1.6 m, the filling ratios of 65%, 70%, 75%, 80%, and 85% were studied. It was found that

the thermal resistance was the smallest at 80% filling ratio, only 0.023 K/W.

(2) The effect of heat transfer distance on thermal performance was investigated at 80% liquid filling ratio. The maximum heat transfer at a distance of 3.7 m is 700 W, and the maximum heat transfer at a distance of 5.7 m is 650 W. At two different heat transfer distances, the thermal resistance first decreases and then gradually stabilizes with the increase of heating power, with the lowest thermal resistances being 0.004 K/W and 0.005 K/W, respectively.

The two-phase loop Thermosiyphon designed in this article demonstrates significant advantages in meeting flexible layout, high heating power heat dissipation, and long-distance heat transport requirements. Provided innovative solutions for future high heating power and distributed thermal management challenges. To further optimize the design and elucidate the underlying mechanisms, future studies are encouraged to employ CFD method to reveal detailed flow patterns, phase-change dynamics, and temperature distributions, thereby enhancing the understanding of thermal-hydraulic performance.

ACKNOWLEDGEMENTS

This study was supported by the Astrometric Reference Frame project, Grant No. JZZX-0103.

CONFLICT OF INTEREST

The authors declare that they have no conflict of interest.

AUTHORS CONTRIBUTION

Yilin Yang: Data analysis, manuscript writing, model optimization. **Yang Liu:** Literature research, numerical simulation, experimental research. **Zhe Yan:** Polished the manuscript and supervised all the work related to the article. **Zhenhua Jiang:** Formal analysis, Polishing of documents.

REFERENCES

Adoni, A. A., Ambirajan, A., Jasvanth, V. S., Kumar, D., & Dutta, P. (2010). Theoretical and experimental studies on an ammonia-based loop heat pipe with a flat evaporator. *IEEE Transactions on Components and Packaging Technologies*, *33*(2), 478-487. https://doi.org/10.1109/TCAPT.2010.2042056

Agostini, F., Gradinger, T., & Cottet, D. (2014). Compact gravity driven and capillary-sized thermosiyphon loop for power electronics cooling. *Journal of Thermal Science and Engineering Applications*, *6*, 031003-1. http://dx.doi.org/10.1115/1.4026184

Armas, G., Rouaze, G., & Marcinichen, J. B. (2021). *Experimental evaluation and simulation validation of an air-cooled loop thermosiyphon designed for high heat load CPUs.* 2021 20th l EEE lntersociety Conference on Themmal and Thermomechanical Phenomena in Electronic Systems (iTherm), 978-1-7281-8539-2/21/$31.00 2021 IEEE. https://doi.org/10.1109/ITherm51669.2021.9503138

Bai, L. Z., Lin, G. P., Wen, D. S., & Feng, J. T. (2009). Experimental investigation of startup behaviors of a dual compensation chamber loop heat pipe with insufficient fluid inventory. *Applied Thermal Engineering*, *29*, 1447-1456. http://dx.doi.org/10.1016/j.applthermaleng.2008.06.019

Cao, Y. W., Guo, C. S., Yu, Y. S., Ma, J., Wu, D. T., & Zou, Y. (2022). Performances of loop heat pipe with the novel bi-porous quaternary MAX phase Ti_3 (Al, Si) C_2 capillary wick. *Vacuum*, *202*, 111185. https://doi.org/10.1016/j.vacuum.2022.111185

Cataldo, F., & Crea, Y. C. (2021). Experimental analysis and modeling of a novel thermosiyphon system for electronics cooling. *Journal of Electronic Packaging*, *143*, 041110-1. https://doi.org/10.1115/1.4052670

Chen, S. J., & Yang, J. (2016). Loop thermosiyphon performance study for solar cells cooling. *Energy Conversion and Management*, *121*, 297-304. http://dx.doi.org/10.1016/j.enconman.2016.05.043

Cheng, P. S., & Wong, S. C. (2024). Detailed visualization experiments on the start-up process and stableoperation of double-layered pulsating heat pipes under vertical andhorizontal orientations. *International Journal of Heat and Mass Transfer*, *231*, 125905. https://doi.org/10.1016/j.ijheatmasstransfer.2024.125905

Guo, H., Ji, X. B., & Xu, J. L. (2020). Enhancement of Loop Heat Pipe Heat Transfer Performance with Superhydrophilic Porous Wick. *International Journal of Thermal Sciences*, *156*, 106466. https://doi.org/10.1016/j.ijthermalsci.2020.106466

He, Y. C., Hu, C. Z., Li, H. Y., Hu, X. F., & Tang, D. W. (2022). Visualized-experimental investigation on a mini-diameter loop thermosiyphon with a wide range of filling ratios. *International Communications in Heat and Mass Transfer*, *133*, 105973. https://doi.org/10.1016/j.icheatmasstransfer.2022.105973

Holman, T. D., Baldauff, R. W., & Khrustalev, D. K. (2020). Stabilized loop heat pipe architecture for reliable operation under high-power transients. *Journal of Thermophysics and Heat Transfer*, *34*(3), 1-8. https://doi.org/10.2514/1.T5790

Hu, H. Z., Chen, C. M., Li, C., & Pan, M. Q. (2023). Experimental investigation of roll bond liquid cooling plates for server chip heat dissipation. *Applied Thermal Engineering*, *226*, 120284. https://doi.org/10.1016/j.applthermaleng.2023.120284

Hua, Y., Qu, J., Yang, W. L., Zhang, T., & Zhao, Y. (2024). Thermal characteristics of a two-phase loop

thermosiyphon with micro-grooved structures inside the evaporator. *International Journal of Heat and Mass Transfer*, *224*, 125357. https://doi.org/10.1016/j.ijheatmasstransfer.2024.125357

Jengsooksawat, S., Rittidech, S., & Booddachan, K. (2014). Loop thermosiyphon with vapour chamber: a thermodynamic Study. *Advances in Mechanical Engineering*, *487191*. http://dx.doi.org/10.1155/2014/487191

Jiao, A. J., Ma, H. B., & Critser J. K. (2007). Evaporation heat transfer characteristics of a grooved heat pipewith micro-trapezoidal grooves. *International Journal of Heat and Mass Transfer*, *50*, 2905-2911. https://doi.org/10.1016/j.ijheatmasstransfer.2007.01.009

Kloczko, S., & Faghri, A. (2020). Experimental investigation on loop thermosiyphon thermal performance with flow visualization. *International Journal of Heat and Mass Transfer*, *150*, 119312. https://doi.org/10.1016/j.ijheatmasstransfer.2020.119312

Li, F. J., Gao, J. M., Shi, X. J., Liang, F., & Tang, R. (2017). Investigation on heat transfer performance of loop thermosiyphonfor inner cooling of motorized spindle. *Journal of Xi'an Jiaotong University*, *51*(7), 8. https://doi.org/10.7652/xjtuxb201707014

Liu, M., Ning, W. J., Yang, J. B., Zhang, Y. K., Han, Z. S., Meng, G., Guo, C. S., Lin, H., & Jia, B. H. (2023). High-performance multi-morphology porous wick fabricated using a composite pore former. *International Communications in Heat and Mass Transfer*, *148*, 107019. https://doi.org/10.1016/j.icheatmasstransfer.2023.107019

Matsubara, K., Tachikawa, S., Kourakata, I., & Matsudaira, Y. (2014). Experiments on thermosiyphon loops for low-temperature waste-heat recovery. *Journal of Thermal Science and Engineering Applications*, *6*, 041006-1. http://dx.doi.org/10.1115/1.4027417

Maydanik, Y. F., & Vershinin, S. V. (2009). Development and tests of ammonia Miniature Loop Heat Pipes with cylindrical evaporators. *Applied Thermal Engineering*, *29*, 2297-2301. https://doi.org/10.1016/j.applthermaleng.2008.11.016

Naik, R., Varadarajan, V., Pundarika, G., & Narasimha, K. R. (2013). Experimental investigation and performance evaluation of a closed loop pulsating heat pipe. *Journal of Applied Fluid Mechanics*, *6*(2), 267-275.

Nakamura, K., Ueno, A., & Nagano, H. (2022). Experimental study on long-distance anti-gravity loop heat pipe with submicron-scale porous structure. *Applied Thermal Engineering*, *214*, 118793. https://doi.org/10.1016/j.applthermaleng.2022.118793

Rukruang, A., Lin, H. Y., Kaew-On, J., & Wang, C. C. (2024). Experimental investigation on thermal performance of multiport minichannel flattened tube thermosiyphon heat exchanger. *Applied Thermal Engineering*, *257*, 124385. https://doi.org/10.1016/j.applthermaleng.2024.124385

Sakthivel, P., Arunkumar, G., Krishnan, P. N., Ramkumar, R., & Parameswaran, P. (2018). Experimental heat transfer analysis on heat pipe using SiO_2 and TiO_2 nano fluid. *Journal of Applied Fluid Mechanics*, *11*, 91-101. http://dx.doi.org/10.36884/jafm.11.SI.29422

Samba, A., Louahlia-Gualous, H., Masson, S. L., & Nörterhäuser, D. (2013). Two-phase thermosiyphon loop for cooling outdoor telecommunication equipments. *Applied Thermal Engineering*, *50*, 1351-1360. https://doi.org/10.1016/j.applthermaleng.2012.05.023

Sarno, C., Tantolin, C., Hodot, R., Maydanik, Y., & Vershinin, S. (2013). Loop thermosiyphon thermal management of the avionics of an in-flight entertainment system. *Applied Thermal Engineering*, *51*, 764-769. http://dx.doi.org/10.1016/j.applthermaleng.2012.10.012

Srivastava, A., Kumar, P., Ambirajan, A., Dutta, P., Varghese, Z., Rohith, B. L., & Subrahmanya, P. (2024). Experimental investigation of thermosiyphons with horizontal evaporatorfor low heat flux applications. *Applied Thermal Engineering*, *257*, 124249. https://doi.org/10.1016/j.applthermaleng.2024.124249

Vasiliev, L., Zhuravlyov, A., Kuzmich, M., & Kulikouski, V. (2022). Development and testing of a novel horizontal loop thermosiyphon as a kW-class heat transfer device. *Applied Thermal Engineering*, *200*, 117682. https://doi.org/10.1016/j.applthermaleng.2021.117682

Venkataramana, P., Vijayakumar, P., & Balakrishna, B. (2022). Experimental investigation of aluminum oxide nanofluid on closed loop pulsating heat pipe performance. *Journal of Applied Fluid Mechanics*, *15*(6), 1947-1955. https://doi.org/10.47176/jafm.15.06.1324

Xu, J. Y., Wang, D. C., Hu, Z. H., Zhang, L., Ye, L., & Zhou, Y. R. (2020). Effect of the working fluid transportation in the copper composite wick on the evaporation efficiency of a flat loop heat pipe. *Applied Thermal Engineering*, *178*, 115515. https://doi.org/10.1016/j.applthermaleng.2020.115515

Zamanifard, A., & Wang, C. C. (2024). An experimental evaluation of the performance of a remote 2U loop thermosiyphon. *Applied Thermal Engineering*, *248*, 123243.

https://doi.org/10.1016/j.applthermaleng.2024.123243

Zhang, H. N., Shao, S. Q., Gao, Y. P., Xu, H. B., & Tian, C. Q. (2020). The effect of heating power distribution on the startup time and overshoot of a loop thermosiyphon with dual evaporators. *Applied Thermal Engineering*, *11651*. https://doi.org/10.1016/j.applthermaleng.2017.12.130

Zhang, P. L., Shi, W. X., Li, X. T., Wang, B. L., & Zhang, G. H. (2017). A performance evaluation index for two-phase thermosiyphon loop used in HVAC systems. *Applied Thermal Engineering*, *11577*. https://doi.org/10.1016/j.applthermaleng.2017.12.056

Zimmermann, A. J. P., & Melo, C. (2014). Two-phase loop thermosiyphon using carbon dioxide applied to the cold end of a Stirling cooler. *Applied Thermal Engineering*, *73*, 549-558. http://dx.doi.org/10.1016/j.applthermaleng.2014.08.004